

Comparative differences of mitral valve-in-valve implantation: A new mitral bioprosthesis versus current mosaic and epic valves

Dee Dee Wang MD^{1,2}  | Brian P. O'Neill MD^{1,2} | Thomas G. Caranasos MD^{1,3} | W. Randolph Chitwood Jr MD^{1,4} | Richard S. Stack MD^{1,5} | William W. O'Neill MD^{1,2}

¹Cardiovascular Masters Consortium, Durham, North Carolina, USA

²Center for Structural Heart Disease, Henry Ford Hospital, Detroit, Michigan, USA

³Department of Surgery, University of North Carolina at Chapel Hill, Chapel Hill, North Carolina, USA

⁴Department of Cardiovascular Sciences, East Carolina University, Greenville, North Carolina, USA

⁵Department of Medicine, Duke University, Durham, North Carolina, USA

Correspondence

Dee Dee Wang, Center for Structural Heart Disease, Henry Ford Hospital, 2799 West Grand Blvd., Clara Ford Pavilion, 439, Detroit, MI 48202, USA.
Email: dwang2@hfhs.org

Funding information

Edwards Lifesciences Corp to Synchrony Labs.

Abstract

Objective: Evaluate transcatheter mitral valve replacement (TMVR) valve-in-valve (VIV) outcomes in three different mitral bioprostheses (of comparable measured internal diameters) under stable hemodynamic and surgical conditions by bench, echocardiographic, computerized tomography (CT), and autopsy comparisons pre- and post-valve implantation in a porcine model under matched controlled conditions.

Background: Impact of surgical bioprosthesis design on TMVR VIV procedures is unknown.

Methods: Fifteen similar-sized Yorkshire pigs underwent pre-procedural CT screening. Twelve had consistent anatomic features and underwent implantation of mitral bioprostheses. Four valves from each of three manufacturers were implanted in randomized fashion: 27-mm Epic, 27-mm Mosaic, and 25-mm Mitris, followed by TMVR VIV with 26 Edwards Sapien3. Post-VIV, suprasternal TEE studies were performed to assess hemodynamic function, followed by a gated contrast CT. After euthanasia, animals underwent necropsy for anatomic evaluation.

Results: All 12 animals had successful VIV implantation with no study deaths. The post vivMitris (3.77 ± 0.36)/(2.2 ± 0.25 mmHg) had the lowest peak/mean trans-mitral gradient and the vivEpic the highest (15.5 ± 2.55)/(7.09 ± 1.13 mmHg). All THVs (transcatheter heart valves) had greatest deformation within the center of the THV frame; with the smallest waist opening area in the vivEpic (329 ± 35.8 mm²) and greatest in the vivMitris (414 ± 33.12 mm²). Bioprosthetic frames without obvious radiopaque markers resulted in the most ventricular implantation of the THV's anteroseptal frame (Epic: -4.52 ± 0.76 mm), versus the most radiopaque bioprosthesis (Mitris: -1.18 ± 2.95 mm), and higher peak LVOT gradients (Epic: 4.82 ± 1.61 mmHg; Mitris: 2.91 ± 1.47 mmHg).

Conclusions: The current study demonstrates marked variations in hemodynamics, THV opening area, and anatomic dimensions among measured similarly sized mitral

Abbreviations: CT, computed tomography; LVOT, left ventricular outflow tract; THV, transcatheter heart valve; TMVR, transcatheter mitral valve replacement; VIV, valve-in-valve.

This is an open access article under the terms of the Creative Commons Attribution-NonCommercial-NoDerivs License, which permits use and distribution in any medium, provided the original work is properly cited, the use is non-commercial and no modifications or adaptations are made.

© 2021 The Authors. *Catheterization and Cardiovascular Interventions* published by Wiley Periodicals LLC.

bioprostheses. These data suggest a critical need for understanding the potential impact of variations in bioprosthesis design on TMVR VIV clinical outcomes.

KEYWORDS

computed tomography, left ventricular outflow tract, transcatheter mitral valve replacement

1 | INTRODUCTION

Bioprosthetic surgical mitral valves have a finite lifespan. Structural deterioration requiring redo mitral valve operation occurs in up-to 35% of patients within 10 years of implantation.^{1,2} Redo mitral valve surgery is associated with high perioperative morbidity and mortality.^{2,3} Given reports of postsurgical redo operation in-hospital mortality rates upwards of 12%, many patients with high STS risk scores are deemed ineligible for redo intervention.^{2,4} In patients with degenerative surgical mitral valves, transcatheter mitral valve replacement (TMVR) valve-in-valve (VIV) options have emerged as safe and feasible alternatives for patients at high operative risk for redo mitral surgery.^{1,4}

Transcatheter mitral valve replacement VIV technology is in its infancy. There are varying modes of structural valve deterioration.⁴ However, there is little published literature on differences in outcomes of TMVR VIV by types of bioprosthesis or mode of degeneration.^{5,6} There is additionally little published literature documenting surgical prosthesis variables that may contribute to the success or failure of TMVR VIV. Surgical prosthesis device sizing and valve selection are still not well understood.⁷ In 2019, the Valve Labeling Taskforce identified inconsistent definitions of surgical prosthesis labeled sizing, inconsistencies between valve sizer dimensions and manufacturer labeled prosthesis sizing as complex issues necessitating important regulatory evaluation.⁷ To date, no recent controlled study has evaluated the acute safety, durability, and function of a standard sized transcatheter heart valve (THV) implanted in similar-sized surgical mitral bioprostheses in a head-to-head comparison study. In human clinical trials and registry data reporting, these studies are not feasible due to the small number of patients anatomically qualifying for TMVR. Additionally, it is difficult for clinical TMVR VIV studies to compare different surgical mitral valve designs in the presence of major human anatomic and hemodynamic variations, variation in modes of structural valve deterioration, and patient-specific co-morbidities. The aim of this controlled preclinical experimental study is to evaluate the outcomes of TMVR VIV in three surgical mitral bioprostheses of comparable measured internal diameters in a head-to-head comparison of acute THV function post-TMVR VIV in the setting of controlled anatomic sizing, hemodynamic conditions, and transcatheter expertise.

2 | METHODS

Between August 2020 and January 2021, 15 Yorkshire pigs underwent anatomical screening for consideration for enrollment

into this study. All animals underwent baseline physical exam screening with on-site veterinary examination at Synchrony Labs (Synchrony Labs LLC, Chapel Hill, NC). This study was supported by Edwards Lifesciences to Synchrony Labs. The funders had no role in the study design, data collection and analysis, decision to publish, or preparation of the manuscript. Study design, evaluation, and implementation were performed by the Cardiovascular Masters Consortium, LLC (CMC). The CMC is an independent group of physicians in the fields of interventional cardiology, interventional imaging, and cardiac surgery who objectively assess new cardiovascular technologies using scientifically designed pre-clinical and clinical studies. The study protocol was approved by the Institutional Animal Care and Use Committee of Synchrony Labs (Synchrony Labs LLC, Durham, NC) and all animals received humane care in compliance with the *Guide for the Care and Use of Laboratory Animals*.⁸

TMVR VIV study primary endpoints were defined according to the Mitral Valve Academic Research Consortium (MVARC) criteria for technical, device, and procedural success.⁶ Secondary endpoints evaluated specific VIV structurally related technical failure and complications. This included presence or absence of any THV structural deformation, device positioning, and TMVR VIV impact on left ventricular outflow tract (LVOT) obstruction (gradient increase ≥ 10 mmHg from baseline).⁶ THV frame deformation was assessed at three points within each device: the atrial portion of the THV, smallest waist of the THV, and the ventricular portion of the THV. The THV opening area was defined as the measured dimensions of the THV stent frame that corresponded to the dimensions of the THV within the bioprosthesis of interest by multi-planar 3D-CT analysis.

2.1 | Animal preparation and examination

Prior to procedural consideration, all animals underwent anatomical screening by contrast-enhanced retrospective electrocardiographic gated computed tomography (CT) scanning with the on-site Siemens scanner (Siemens Dual Somatom, Siemens Medical, Forchheim, Germany).⁹ Pre-procedural screening focused on anatomical characteristics relevant to physicians in the clinical setting. These data focused on left atrial size, mitral annulus dimensions, left ventricular function, and potential transseptal catheter crossing height. Those animals with transseptal crossing heights ≤ 15 mm or mitral annular dimensions with $>6\%$ variation from other study animals were excluded. Twelve pigs met study inclusion criteria.

We performed bench measurements of all labeled sizes of mitral bioprostheses of interest, the Epic (Abbott, Abbott Park, IL), Mosaic (Medtronic, Minneapolis, MN), and Mitris (Edwards Lifesciences, Irvine, CA) valves (Figure S1 and Table S1). Inner to inner surgical frame dimensions were captured at multiple levels within the bioprosthesis frame. Surgical valve size selection was determined based on grouping of similar internal bioprosthesis frame dimensions, and not manufacturer labeled device sizing.¹⁰

Surgical bioprosthesis implantation was performed same day of VIV TMVR by two surgeons blinded to the type of surgical prosthesis being implanted until time of surgical procedure.¹⁰ Until time of THV implantation, the two implanting interventional cardiologists (BPO, WWO) were blinded to type of surgical prosthesis to be implanted in each procedure. Surgical valves were performed in randomized order between the interventional cardiologists with all three valves implanted by each interventionalist to minimize operator variability for all three surgical mitral bioprostheses. Echocardiographic, suprasternal TEE, and periprocedural CT imaging was performed by the same interventional imaging physician across all three TMVR VIV procedures in all phases of device interrogation utilizing the 27-mm Abbott Epic, the 27-mm Medtronic Mosaic, and the 25-mm Edwards Mitris.

2.2 | TMVR VIV procedure

VIV TMVR was performed according to previously published techniques for transseptal mitral VIV.¹¹ All animals underwent transseptal access via suprasternal TEE probe guidance and received intravenous heparin during the procedure to maintain an activated clotting time > 250 s. Under fluoroscopic and TEE guidance, the THV was positioned within the confines of the surgical mitral bioprosthesis to minimize any risk of LVOT obstruction and deployed under rapid pacing with slow controlled balloon inflation.¹¹ The same VIV delivery technique and balloon inflation methodology was applied across all implanted THV.

2.3 | Post-TMVR VIV evaluation

Epicardial echocardiograms were obtained according to standard of care guidelines according to the American Society of Echocardiography recommendations.¹² Suprasternal echocardiographic imaging was performed using a standard TEE probe inserted via suprasternal cutdown posterior to the cardiac silhouette. To ensure reproducibility of all echocardiographic evaluation, hemodynamic stability was maintained for all studies, with an effort to capture all study variables at similar heart rate, and blood pressure points. Following TMVR VIV procedure, all study animals were transported to on-site Siemens CT scanner for a contrast ECG-gated retrospective scan for evaluation of THV function, post-TMVR VIV neo-LVOT, and assessment of device landing zone utilizing previously described methodologies.¹³

2.4 | Data collection and statistics

Pre-procedure (anesthetized but unoperated) multi-detector retrospectively gated contrast enhanced CT scans were performed on all animals. Multiphasic CT image reconstructions were performed at 1.5-mm intervals. Images were transferred in DICOM (Digital Imaging and Communications in Medicine) format to off-line computer stations for further processing. CT segmentation and analysis was performed using Vitrea (Vital Images, Minnetonka, MN) and Mimics (Materialise, Leuven, Belgium) software. All study animals were euthanized and underwent on-site supervised necropsy with cardiac explantation for anatomical evaluation of each THV. Given the small sample size, descriptive data are presented with no further statistical analysis. Continuous and categorical variables are defined as mean and standard deviation; discrete variables are presented as numbers and percentages.

3 | RESULTS

Fifteen animals underwent rigorous pre-procedural CT anatomical screening. All animals were screened to ensure the most accurate anatomic sizing of key cardiac chambers, mitral annulus dimensions, and feasibility of transseptal crossing height for VIV TMVR. Three animals were excluded due to >6% variation of mitral annular dimensions, or transseptal crossing height \leq 15 mm as evaluated by CT.

3.1 | Study population characteristics

Baseline animal procedural anatomical evaluation parameters are documented in Table 1. There was <6% anatomical variation among all study animals. The mean mitral annulus area was 1410.00 ± 133.60 mm², with mean left atrial width of 43.64 ± 2.08 mm, left atrial height of 28.87 ± 1.93 mm, and mean transseptal crossing height of 20.53 ± 1.48 mm. Mean commissure to commissure distance of native mitral annuli was 41.56 ± 1.82 mm, with mean anterior to posterior distance of 37.78 ± 1.72 mm.

Baseline post-surgical bioprosthesis hemodynamic and echocardiographic data were similar among all 12 study animals (Table 2). Post-surgical bioprosthesis mitral valve peak gradients averaged 7.23 ± 3.38 mmHg, mean gradient 3.82 ± 1.76 mmHg, and LVOT peak gradients averaged 3.29 ± 1.42 mmHg (mean 1.54 ± 0.60 mmHg). All study animals had normal LV function at post-surgical valve implant (Table 2). By epicardial echocardiographic evaluation, no animal had underlying evidence of LVOT obstruction. Three of four Epic bioprostheses were noted to have an eccentric paravalvular leak at the anterolateral commissure. All other post-implantation mitral bioprostheses had no central or paravalvular leaks. All mitral bioprostheses were noted to have normal leaflet function and coaptation without evidence of stenosis. All TMVR VIV procedures achieved device implantation technical success; there were no valve embolizations.

TABLE 1 Baseline porcine demographic information and CT screening anatomical information

| | Epic | Mosaic | Mitris |
|---|--|--|-----------------------|
| Age at implant (days) | 169.8 ± 27.2 | 165.5 ± 22.8 | 148.8 ± 7.6 |
| Weight at implant (kg) | 88.0 ± 8.95 | 89.3 ± 6.26 | 85.0 ± 6.89 |
| Mitral annulus area (sq mm) | 1436.75 ± 131.18 (vs. Mitris 1.5% variation) | 1349.00 ± 100.62 (vs. Mitris 4.79%) | 1415.25 ± 152.02 |
| Mitral annulus circumference (mm) | 139 ± 7.75 (vs. Mitris 1.45% variation) | 133.75 ± 5.38 (vs. Mitris 2.40% variation) | 137.0 ± 7.53 |
| Mitral annulus commissure to commissure distance (mm) | 42.70 ± 1.23 (vs. Mitris 2.01% variation) | 40.35 ± 1.31 (vs. Mitris 3.65% variation) | 41.85 ± 2.72 |
| Mitral annulus anterior to posterior distance (mm) | 37.35 ± 1.79 (vs. Mitris 0.75% variation) | 38.1 ± 1.0 (vs. Mitris 1.24% variation) | 37.63 ± 2.27 |
| Left atrium width (mm) | 43.13 ± 2.79 (vs. Mitris 0.30% variation) | 44.80 ± 1.40 (vs. Mitris 4.10% variation) | 43.0 ± 2.20 |
| Left atrium height (mm) | 28.35 ± 1.12 (vs. Mitris 0.46% variation) | 29.78 ± 3.17 (vs. Mitris 4.46% variation) | 28.48 ± 1.41 |
| Transseptal crossing height (mm) | 19.80 ± 1.49 (vs. Mitris 5.55% variation) | 20.85 ± 1.36 (vs. Mitris 0.38% variation) | 20.93 ± 1.90 |
| Frequency of circumflex artery coursing close to mitral annulus | One out of four pigs | Two out of four pigs | Four out of four pigs |

Note: From Wang et al.¹⁰

TABLE 2 Hemodynamics at time of echocardiographic data capture with concomitant baseline post-surgical implantation echocardiographic measurements

| | EPIC | Mosaic | MITRIS |
|-----------------------------------|---|---|---------------|
| Post-surgical valve implant | | | |
| Systolic blood pressure | 92.5 ± 9.85 (vs. Mitris 0.53% variation) | 91.25 ± 8.81 (vs. Mitris 1.9% variation) | 93 ± 12.65 |
| Diastolic blood pressure | 59.0 ± 7.53 | 64.75 ± 8.73 | 62.5 ± 8.96 |
| Heart rate | 92.5 ± 11.27 (vs. Mitris 3.9% variation) | 89.8 ± 9.29 (vs. Mitris 0.89% variation) | 89.0 ± 10.55 |
| Left ventricle ejection fraction | >55% | >55% | >55% |
| Mitral valve peak gradient (mmHg) | 9.17 ± 3.72 | 7.2 ± 4.11 | 5.05 ± 2.67 |
| Mitral valve mean gradient (mmHg) | 4.59 ± 1.90 | 3.92 ± 2.40 | 2.61 ± 1.26 |
| LVOT peak gradient | 3.42 ± 1.31 | 4.40 ± 1.25 | 2.06 ± 1.05 |
| LVOT mean gradient | 1.72 ± 0.63 | 1.86 ± 0.47 | 1.04 ± 0.55 |
| Post-TMVR VIV implant | | | |
| Systolic blood pressure | 86.25 ± 14.57 (vs. Mitris 2.3% variation) | 81.75 ± 13.87 (vs. Mitris 7.6% variation) | 88.25 ± 11.5 |
| Diastolic blood pressure | 53.25 ± 5.25 | 50.75 ± 11.62 | 44.25 ± 6.9 |
| Heart rate | 95.5 ± 11.68 (vs. Mitris 6.2% variation) | 85.75 ± 9.25 (vs. Mitris 4.6% variation) | 89.75 ± 12.31 |

Note: Data from post-surgical valve implant are from Wang et al.¹⁰

3.2 | Comparison of valve prosthesis type: Major safety, technical, and mechanistic endpoints

3.2.1 | Imaging measurements

Post-TMVR VIV echocardiographic findings are depicted in Table 3. Among the three types of mitral bioprostheses, the TMVR VIV in the 27 mm-Epic (vivEpic) had the highest peak/mean mitral gradient, followed by the TMVR VIV in 27-mm Mosaic (vivMosaic), while the TMVR VIV in the 25-mm Mitris (vivMitris) had the least mitral peak/mean gradient (Table 3). There was no evidence of paravalvular leak between the frame of the implanted THV and the surgical bioprosthesis on any implant.

Transcatheter heart valve frame dimensions were obtained at multiple levels by multi-planar 3D reconstruction of the post-TMVR VIV CT images (Table 3). THV frame dimensions were documented at the atrial opening of the THV, the narrowest portion of the THV frame defined as the “waist” of the THV within the surgical mitral bioprosthesis, and again at the most ventricular portion of the frame of the THV in the LVOT.

THV frame dimensions impacted transmitral Doppler echocardiographic gradients. Multi-planar 3D CT images demonstrated the vivEpic to have the smallest THV atrial opening area (396.00 ± 42.88 mm²), smallest THV waist opening area (329.00 ± 35.8 mm²), and the highest peak/mean mitral gradient (15.50 ± 2.55)/(7.09 ± 1.13 mmHg). The vivMitris had the largest THV opening area (428.00 ± 47.9 mm²), largest THV waist opening area (414.00

TABLE 3 Transcatheter valve function post TMVR VIV

| | EPIC (27 mm) | Mosaic (27 mm) | MITRIS (25 mm) |
|---|---------------|----------------|----------------|
| TMVR VIV atrial opening max internal dimensions (mm) | 21.8 ± 1.06 | 22.3 ± 0.88 | 22.85 ± 0.91 |
| TMVR VIV atrial opening min internal dimensions (mm) | 21.06 ± 1.33 | 21.58 ± 1.09 | 22.53 ± 0.83 |
| TMVR VIV atrial opening surface area (mm ²) | 396 ± 42.88 | 414.5 ± 27.96 | 428 ± 47.9 |
| TMVR VIV atrial opening circumference (mm) | 70.5 ± 3.79 | 72.5 ± 2.52 | 73.5 ± 4.20 |
| TMVR VIV waist max internal dimensions (mm) | 20.03 ± 1.05 | 20.5 ± 0.25 | 22.48 ± 1.24 |
| TMVR VIV waist minimal internal dimensions (mm) | 19.6 ± 0.70 | 19.98 ± 0.56 | 21.7 ± 0.82 |
| TMVR VIV waist opening surface area (mm ²) | 329 ± 35.80 | 347 ± 17.66 | 414 ± 33.12 |
| TMVR VIV waist opening circumference (mm) | 64.25 ± 3.59 | 66 ± 1.83 | 72 ± 3.16 |
| TMVR VIV ventricular opening max internal dimensions (mm) | 24.0 ± 1.13 | 23.95 ± 0.56 | 23.75 ± 0.58 |
| TMVR VIV ventricular opening min internal dimensions (mm) | 23.38 ± 0.50 | 22.68 ± 1.36 | 23.45 ± 0.93 |
| TMVR VIV ventricular opening area (mm ²) | 471.5 ± 39.52 | 468.25 ± 39.02 | 473.5 ± 27.87 |
| TMVR VIV ventricular opening circumference (mm) | 77 ± 2.94 | 76.75 ± 2.99 | 77.25 ± 2.22 |
| Post TMVR VIV mitral peak gradient (mmHg) | 15.5 ± 2.55 | 9.97 ± 3.19 | 3.77 ± 0.36 |
| Post TMVR VIV mitral mean gradient (mmHg) | 7.09 ± 1.13 | 5.32 ± 1.31 | 2.2 ± 0.25 |

Note: Transcatheter valve dimensions by CT versus Doppler parameters of TMVR VIV function (see corresponding Figure 1).

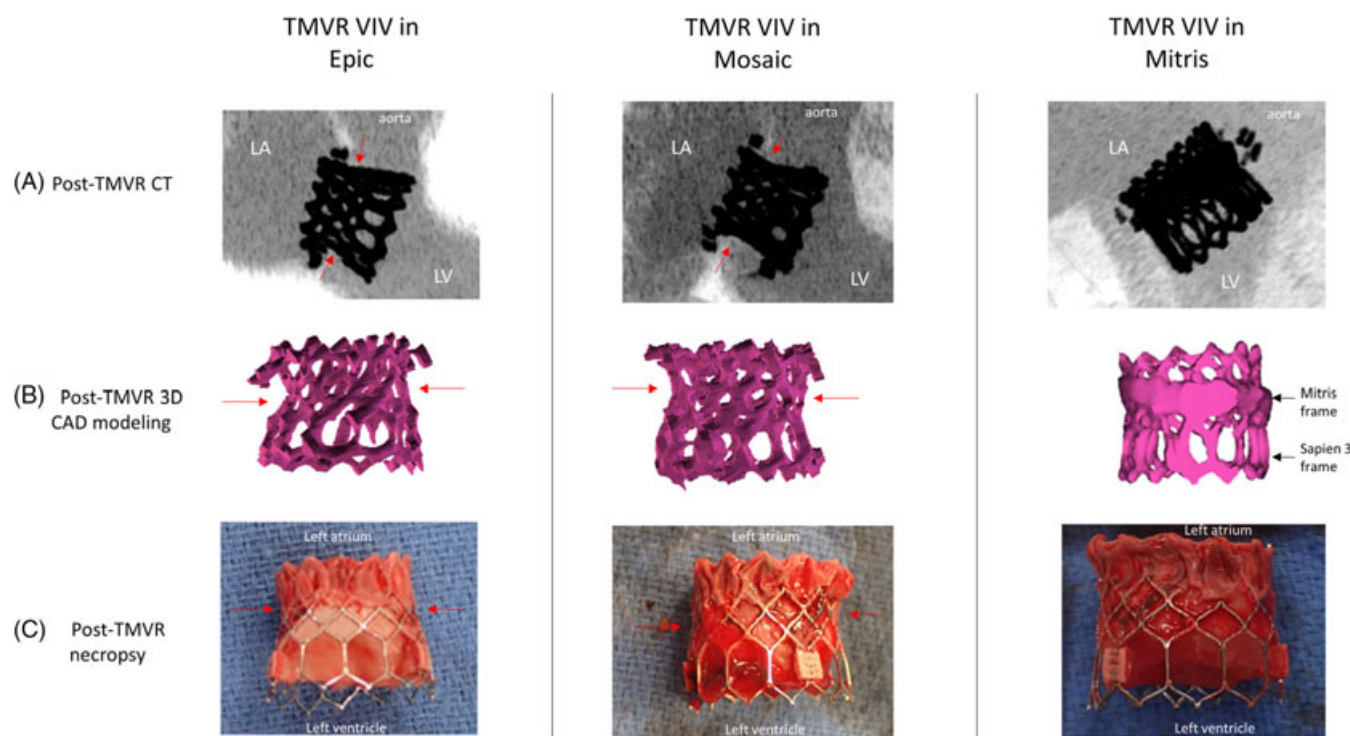


FIGURE 1 Post-TMVR VIV variation in 26S3 frame expansion among different bioprostheses. Row (A) demonstrates greater restriction of the 26S3 THV's ability to fully expand within its atrial dimensions in the Epic and the Mosaic as compared to the Mitris bioprosthesis. Row (B) demonstrates the 3D contour and constraint at the waist (red arrow) of the 26S3 that is present more prominently in the Epic and Mosaic bioprostheses as compared to the Mitris. Row C necropsy images of the explanted 26S3 confirms the post-TMVR VIV CT findings demonstrating atrial and waist landing zone constraint of the THV in different bioprostheses. CAD, computer-aided-design; LA, left atrium; LV, left ventricle; THV, transcatheter heart valve; TMVR, transcatheter mitral valve replacement; VIV, valve-in-valve [Color figure can be viewed at wileyonlinelibrary.com]

TABLE 4 TMVR VIV depth of protrusion versus hemodynamics

| | Epic (27 mm) | Mosaic (27 mm) | Mitris (25 mm) |
|--|----------------|----------------|----------------|
| Transcatheter heart valve depth of protrusion in LV at anteroseptal surgical strut (mm) | -4.52 ± 0.76 | -4.19 ± 0.85 | -1.18 ± 2.95 |
| Transcatheter heart valve depth of protrusion in LV at anterolateral surgical strut (mm) | -4.37 ± 2.98 | -1.26 ± 0.59 | -0.27 ± 2.88 |
| Transcatheter heart valve depth of protrusion in LV at posterior surgical strut (mm) | -2.29 ± 1.64 | -2.78 ± 1.08 | -0.53 ± 2.18 |
| Predicted VIV Neo-LVOT area (in mm ²) | 247.34 ± 31.0 | 223.22 ± 26.42 | 225.07 ± 56.63 |
| Actual post post-TMVR VIV Neo-LVOT area (in mm ²) | 191.06 ± 34.76 | 191.16 ± 6.0 | 201.47 ± 40.57 |
| Difference in predicted and actual post-TMVR VIV Neo-LVOT area (in mm ²) | -56.28 ± 40.93 | -32.06 ± 25.80 | -23.6 ± 24.72 |
| LVOT peak gradient (mmHg) | 4.82 ± 1.61 | 3.54 ± 1.30 | 2.91 ± 1.47 |
| LVOT mean gradient (mmHg) | 2.32 ± 0.62 | 1.57 ± 0.60 | 1.32 ± 0.55 |

Note: Comparative evaluation of post transcatheter valve-in-valve left ventricular outflow tract risk (see corresponding Figure 2). Abbreviations: LV, left ventricle; LVOT, left ventricular outflow tract; VIV, valve-in-valve.

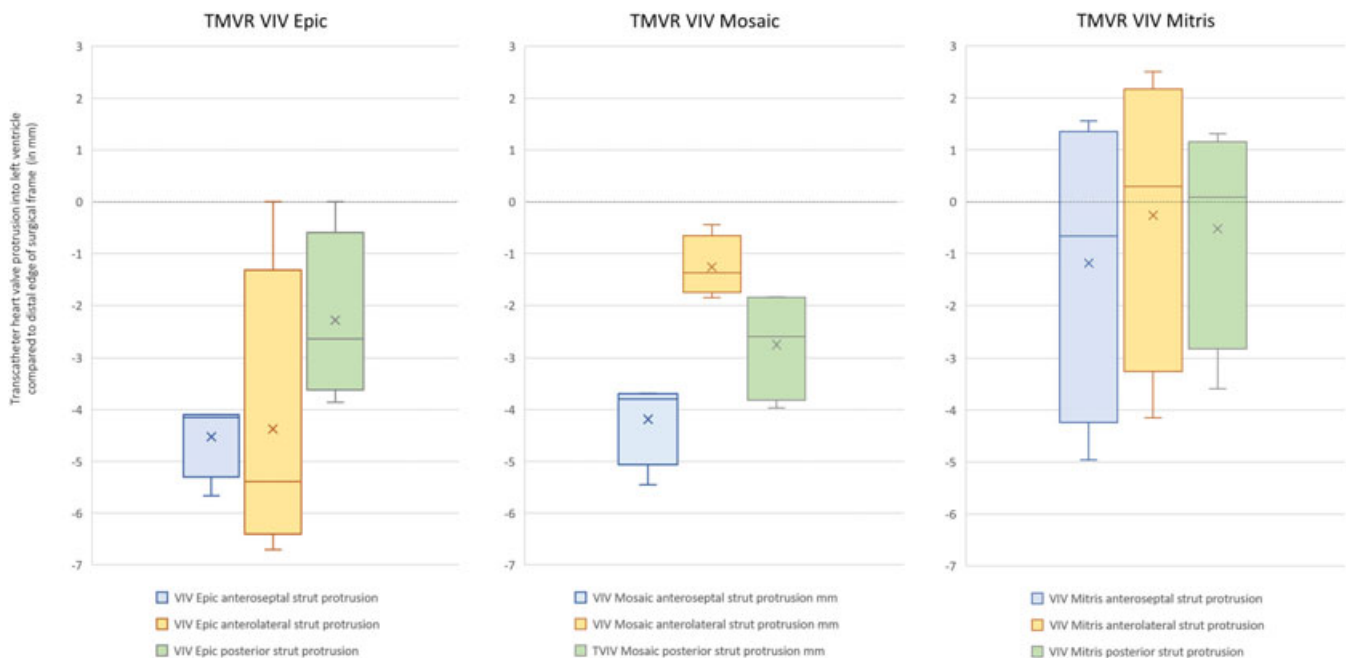


FIGURE 2 Consistency of TMVR VIV deployment landing zone versus type of bioprosthesis. The TMVR VIV Epic implantation trended toward greater protrusion into the LVOT across all three surgical struts as compared to the Mosaic and the Mitris bioprostheses. The TMVR VIV in Mitris demonstrated greatest ability to land within the depth of the bioprosthesis frame across all three surgical struts. Letter 'x' within each plot depicts the mean marker. TMVR, transcatheter mitral valve replacement; VIV, valve-in-valve [Color figure can be viewed at wileyonlinelibrary.com]

± 33.12 mm²), and the lowest peak/mean mitral gradient (3.77 ± 0.36)/(2.20 ± 0.25 mmHg; Figure 1). Compared to the vivEpic and vivMosaic, the vivMitris was the only THV noted to have a decrease in mitral peak/mean gradient post-VIV (3.77 ± 0.36)/(2.20 ± 0.25 mmHg) compared to immediate postsurgical bioprosthesis implantation without VIV (5.05 ± 2.67)/(2.61 ± 1.26 mmHg). All other VIV prostheses were noted to have an increase between post-surgical and post-TMVR VIV mitral peak/mean gradients.

3.2.2 | Risk of LVOT obstruction measures

There was no clinically significant LVOT obstruction in any study animal post-TMVR VIV. Post-TMVR VIV predicted neo-LVOT area was performed using a 26 Sapien 3 heart valve modeled at depth of deployment flush with the distal strut of each mitral bioprosthesis. The predicted neo-LVOT and the actual TMVR VIV deployment were intended to be at the same landing zone. Post-VIV procedure, actual

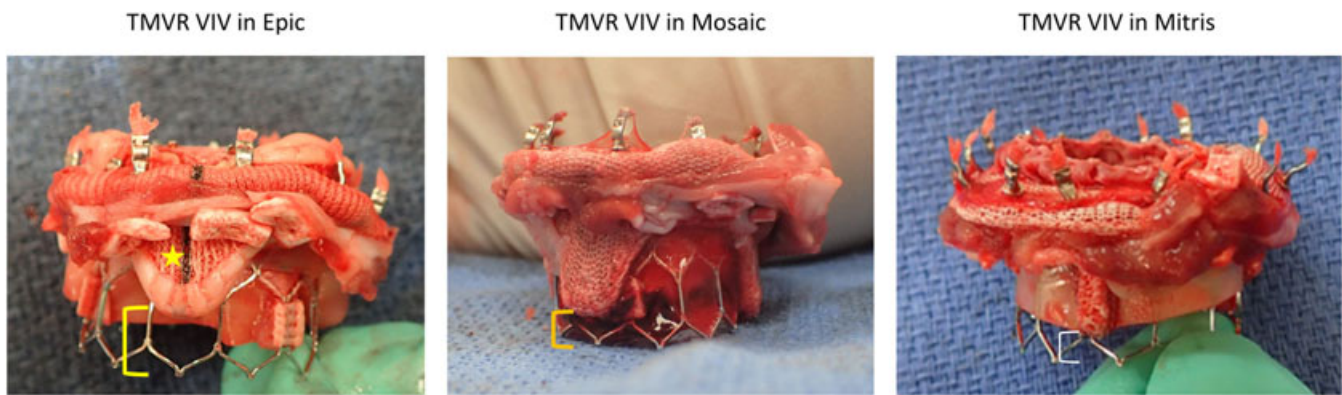
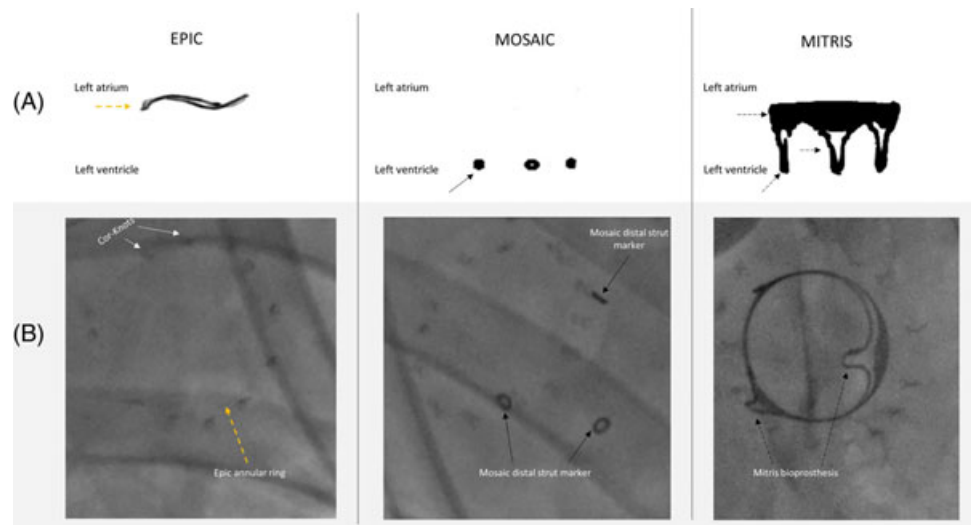


FIGURE 3 Variations in bioprosthesis strut design and impact on TMVR VIV. Pictured on the far left, the TMVR device (yellow bracket) has greater ventricular protrusion beyond the distal portions of the Epic bioprosthesis as compared to the Mosaic (orange bracket) and Mitris bioprostheses (white bracket). The Epic bioprosthesis demonstrates a wider strut (yellow star) width than the Mosaic and Mitris bioprostheses. VIV, valve-in-valve [Color figure can be viewed at [wileyonlinelibrary.com](https://onlinelibrary.wiley.com)]

FIGURE 4 Fluoroscopic visibility of each type of bioprosthesis. Row (A) demonstrates the different bioprostheses' fluoroscopic visibility by CT. The Epic bioprosthesis has a light annular rim (orange dashed arrow) visible at its atrial portion of the mitral cuff, the Mosaic has radiopaque circles (black arrows) within each distal strut. The entire Mitris frame is radiopaque (black dashed arrows) and visible under fluoroscopy. Row (B) demonstrates the presence or absence of fluoroscopic landmarks of each bioprosthesis [Color figure can be viewed at [wileyonlinelibrary.com](https://onlinelibrary.wiley.com)]



neo-LVOT area was performed using the final landing zone of the THV. Additionally, 3D multi-planar CT reconstruction was performed to analyze the depth of transcatheter heart frame stent deployment at the level of the surgical anteroseptal, anterolateral, and posterior struts within the LVOT (Table 4).

There was variability in depth of THV implantation among all three struts of the surgical mitral bioprostheses. All THVs trended toward having a more ventricular deployment at the level of the anteroseptal strut (Figure 2). The vivEpic had the most ventricular protrusion of the THV frame at the anteroseptal (-4.52 ± 0.76 mm), anterolateral (-4.37 ± 2.98 mm), posterior struts (-2.29 ± 1.64 mm), and highest peak LVOT gradient (4.82 ± 1.61 mmHg). The vivMitris had the least amount of protrusion beyond the frame of the surgical prosthesis struts (anteroseptal strut: -1.18 ± 2.95 mm, anterolateral strut: -0.27 ± 2.88 , posterior strut: -0.53 ± 2.18 mm), and smallest peak LVOT gradient (2.91 ± 1.47 mmHg). Visual inspection of the THV at necropsy confirmed multi-planar CT reconstruction findings (Figure 3).

3.3 | Bench measurements: Bioprosthesis design and impact on THV function

Surgical prosthesis frame pre-VIV TMVR dimensions were additionally obtained at the level of the sewing ring, and the ventricular portion of the surgical frame (Table S1). Bench surgical prosthesis dimensions demonstrated the 27-mm Epic to have the smallest atrial internal dimensions at the level of the sewing cuff (22×22 mm), corresponding to the small post-VIV TMVR atrial frame dimensions (max internal dimension: 21.8 ± 1.06 mm, min internal dimension: 21.06 ± 1.33 mm). Corresponding associations between size of surgical frame atrial sewing cuff internal dimensions and ability of post-VIV THV atrial dimensions to expand remained consistent on CT evaluation (Table 3; Table S1).

Multiple analyses of surgical strut design were recorded. Bench measurements of surgical strut dimensions were obtained (Table S2). There were no obvious identifiable trends between length of surgical strut protruding into the LVOT and post-TMVR VIV LVOT peak/

mean gradients. Fluoroscopic evaluation of surgical prosthesis and strut design demonstrated variation in prosthesis visibility. In descending order, the most challenging VIV TMVR deployment was in the least fluoroscopically visible 27-mm Epic prosthesis, followed by the 27-mm Mosaic, and most visible was the 25-mm Mitris (Figure 4). Presence of radiopaque distal strut markers and radiopaque frame was associated with more consistency between predicted and actual post-TMVR VIV neo-LVOT areas (Figure 4 and Table 4).

4 | DISCUSSION

Porcine models have been utilized extensively for preclinical evaluation of prosthetic valve design.^{14–16} This is the first preclinical head-to-head evaluation of TMVR VIV utilizing a 26 Sapien 3 THV across three different surgical prosthesis design platforms in a controlled anatomic and hemodynamic environment.

Here, we show that there was a strong connection between (1) transcatheter heart valve atrial and waist opening area to post-TMVR VIV mitral peak/mean gradients, (2) surgical internal frame dimensions to the degree of THV expansion, and (3) fluoroscopic visibility of mitral bioprostheses compared to post-TMVR VIV LVOT peak gradient. The 27-mm Epic mitral bioprosthesis, with smallest internal atrial dimensions, subsequently had the most constrained and narrowing of the inflow of the atrial dimensions of the THV in the Epic, and even smaller vivEpic waist THV dimensions, leading to the highest post-TMVR VIV mitral peak/mean gradients. Absence of radiopaque markers in the distal struts of the Epic bioprosthesis impaired visualization of TMVR VIV landing zones, resulting in greater risk of ventricular implantation of the THV beyond intended TMVR VIV landing zone. This lack of fluoroscopic visibility resulted in the 27-mm Epic device trending toward higher peak LVOT gradients, than similar-sized prostheses that had radiopaque distal strut demarcated landing zones.

Current TMVR VIV literature observed higher post-VIV mitral mean gradients to be associated with worse clinical outcomes.^{4,17} In the VIVID registry, fewer TMVR VIV devices met the MVARC device success criteria primarily due to findings of transmitral mean gradients ≥ 5 mmHg post-TMVR VIV.⁵ Patients with post-TMVR VIV mitral mean gradients ≥ 10 mmHg were noted to have higher likelihood of developing clinical symptoms of heart failure and needing reintervention.⁵ Discrepancies in post-VIV mitral mean gradient were thought to be attributed to the size of THV implanted in the degenerated bioprosthesis, resulting in suboptimal hemodynamic outcomes, or suboptimal expansion of the THV leading to frozen leaflets, and less so on surgical frame design.^{5,17} To date, there is little published literature on the impact of surgical frame design on structural deterioration of the implanted THV.

This study is the first to demonstrate that variations in surgical bioprosthesis frame shape, frame radiopacity, and internal frame sizing can all directly impact the form and function of the implanted THV. Surgical mitral bioprostheses that were more tubular in shape such as the 25-mm Mitris, had more uniformity in expansion of the 26 Sapien

3 THV within the bioprosthesis, resulting in more laminar flow, optimal THV leaflet opening, less THV leaflet pinwheeling, and smaller post-VIV mitral peak/mean gradient than its counterpart the 27-mm Epic and 27-mm Mosaic prostheses.

Modern mechanisms of transcatheter structural heart valve deterioration have been primarily attributed to presence or absence of long-term intake of oral anticoagulation.¹⁷ This is the first study to demonstrate, in the absence of any surgical valve structural deterioration, while on therapeutic anticoagulation, the controlled implantation of a 26 Sapien 3 was independently associated with higher peak/mean mitral gradients in the 27-mm Epic, followed by the 27-mm Mosaic, followed by the 25-mm Mitris. Hence, by default, in the absence of existing structural valve deterioration, variations in mitral peak/mean gradients post-VIV are likely due to differences in surgical device design. In the absence of standardized guidelines on surgical bioprostheses' sizing, design, and device selection, physicians must consider each patient's likelihood of requiring a redo VIV procedure upon surgical structural valve degeneration prior to mitral bioprosthesis implantation. Failure to account for the impact of surgical valve design on future TMVR VIV procedures may increase a patient's risk of early VIV structural degeneration.

5 | LIMITATIONS

This acute animal study is limited by small sample size without ability to assess for long-term VIV durability. In the absence of frozen leaflets, findings of elevated transmitral peak/mean gradients secondary to structural constraints within the surgical bioprostheses have unknown long-term clinical impact. This study demonstrates greater velocities, and greater resulting turbulent flow in VIV prosthesis with the least tubular expansion. To date, the relationship between turbulent Doppler velocities and calculated echocardiographic gradients on long-term clinical outcomes of THVs is not yet established. Although this study rigorously accounted for reproducible anatomic and hemodynamic parameters, it serves as a potential outline for future human clinical studies. Given the small number of animals in this pilot study, all study results should be interpreted as hypothesis generating. Larger sample size study populations with long-term follow-up will be necessary to evaluate clinical outcomes.

6 | CONCLUSION

The impact of surgical prosthesis designs on transcatheter mitral VIV biomechanical and hemodynamic function is not well studied. Heterogeneity in surgical prosthesis design may positively or negatively affect THV structural form and function. Mitral bioprosthesis device selection must consider the patients' potential candidacy for future TMVR VIV procedures upon structural valve deterioration. Implications of this study demonstrate a critical need for standardization and scientific evaluation of the impact of surgical bioprosthesis design on TMVR VIV function to ensure optimal outcomes for clinical human implantation.

ACKNOWLEDGMENTS

This study was supported by Edwards Lifesciences Corp to Synchrony Labs. The funders had no role in study design, data collection and analysis, decision to publish, or preparation of the manuscript. The authors attest that they had full freedom to explore the data, independently analyze the results and submit the material for publication.

CONFLICT OF INTEREST

Dee Dee Wang, MD: Consultant for Edwards Lifesciences, Boston Scientific, Abbott, Neochord. Boston Scientific Research grant support assigned to employer Henry Ford Health System. Member of Cardiovascular Masters Consortium (outside consultants to Synchrony Labs for this study) and Structural Heart Imaging LLC. Thomas G. Caranasos, MD: Member of Cardiovascular Masters Consortium (outside consultants to Synchrony Labs for this study), proctor for Atricure, proctor for Cryolife. Brian P. O'Neill, MD: Consultant to and receives research support from Edwards Lifesciences. Member of Cardiovascular Masters Consortium (outside consultants to Synchrony Labs for this study). Richard S. Stack, MD: Member of Cardiovascular Masters Consortium (outside consultants to Synchrony Labs for this study), Synchrony Labs (a wholly owned subsidiary of Synecor LLC), Structural Heart Imaging LLC. William W. O'Neill, MD: Member of Cardiovascular Masters Consortium (outside consultants to Synchrony Labs for this study), Synchrony Labs (a wholly owned subsidiary of Synecor LLC), Structural Heart Imaging LLC. W. Randolph Chitwood Jr., MD: Consultant for Neochord, Medtronic, Member of Cardiovascular Masters Consortium (outside consultants to Synchrony Labs for this study).

DATA AVAILABILITY STATEMENT

The data that supports the findings of this study are available in the supplementary material of this article

ORCID

Dee Dee Wang  <https://orcid.org/0000-0002-5784-9924>

REFERENCES

1. Aalaei-Andabili SH, Bavry AA, Petersen J, et al. Transcatheter mitral valve-in-valve and valve-in-ring replacement: lessons learned from bioprosthetic surgical valve failures. *J Card Surg.* 2021;36:4024-4029.
2. Vohra HA, Whistance RN, Roubelakis A, et al. Outcome after redo-mitral valve replacement in adult patients: a 10-year single-Centre experience. *Interact Cardiovasc Thorac Surg.* 2012;14:575-579.
3. Mehaffey HJ, Hawkins RB, Schubert S, et al. Contemporary outcomes in reoperative mitral valve surgery. *Heart.* 2018;104:652-656.
4. Guerrero M, Pursnani A, Narang A, et al. Prospective evaluation of transseptal TMVR for failed surgical bioprostheses: MITRAL trial valve-in-valve arm 1-year outcomes. *JACC Cardiovasc Interv.* 2021;14:859-872.
5. Simonato M, Whisenant B, Ribeiro HB, et al. Transcatheter mitral valve replacement after surgical repair or replacement: comprehensive midterm evaluation of valve-in-valve and valve-in-ring implantation from the VIVID registry. *Circulation.* 2021;143:104-116.
6. Stone GW, Adams DH, Abraham WT, et al. Clinical trial design principles and endpoint definitions for transcatheter mitral valve repair and replacement: part 2: endpoint definitions: a consensus document from the mitral valve academic research consortium. *J Am Coll Cardiol.* 2015;66:308-321.

7. Durko AP, Head SJ, Pibarot P, et al. Characteristics of surgical prosthetic heart valves and problems around labeling: a document from the European Association for Cardio-Thoracic Surgery (EACTS)-the Society of Thoracic Surgeons (STS)-American Association for Thoracic Surgery (AATS) valve labelling task force. *J Thorac Cardiovasc Surg.* 2019;158:1041-1054.
8. National Research Council. *Guide for the Care and Use of Laboratory Animals.* 8th ed. National Academies Press; 2011.
9. Lipiski M, Eberhard M, Fleischmann T, et al. Computed tomography-based evaluation of porcine cardiac dimensions to assist in pre-study planning and optimized model selection for pre-clinical research. *Sci Rep.* 2020;10:6020.
10. Wang DD, Caranasos TG, O'Neill BP, Stack RS, O'Neill WW, Chitwood WR. Comparison of a new bioprosthetic mitral valve to other commercially available devices under controlled conditions in a porcine model. *J Card Surg.* 2021;36(12):4654-4662. doi:10.1111/jocs.16021
11. Guerrero M, Salinger M, Pursnani A, et al. Transseptal transcatheter mitral valve-in-valve: a step by step guide from preprocedural planning to post-procedural care. *Catheter Cardiovasc Interv.* 2018;92:E185-E196.
12. Zoghbi WA, Chambers JB, Dumesnil JG, et al. Recommendations for evaluation of prosthetic valves with echocardiography and doppler ultrasound: a report From the American Society of Echocardiography's Guidelines and Standards Committee and the Task Force on Prosthetic Valves, developed in conjunction with the American College of Cardiology Cardiovascular Imaging Committee, Cardiac Imaging Committee of the American Heart Association, the European Association of Echocardiography, a registered branch of the European Society of Cardiology, the Japanese Society of Echocardiography and the Canadian Society of Echocardiography, endorsed by the American College of Cardiology Foundation, American Heart Association, European Association of Echocardiography, a registered branch of the European Society of Cardiology, the Japanese Society of Echocardiography, and Canadian Society of Echocardiography. *J Am Soc Echocardiogr.* 2009;22:975-1014.
13. Wang DD, Eng MH, Greenbaum AB, et al. Validating a prediction modeling tool for left ventricular outflow tract (LVOT) obstruction after transcatheter mitral valve replacement (TMVR). *Catheter Cardiovasc Interv.* 2018;92:379-387.
14. Li D, Ren BH, Shen Y, et al. A Swine model for long-term evaluation of prosthetic heart valves. *ANZ J Surg.* 2007;77:654-658.
15. Grehan JF, Hilbert SL, Ferrans VJ, Droel JS, Salerno CT, Bianco RW. Development and evaluation of a swine model to assess the preclinical safety of mechanical heart valves. *J Heart Valve Dis.* 2000;9:710.
16. Smerup M, Pedersen TF, Nyboe C, et al. A long-term porcine model for evaluation of prosthetic heart valves. *Heart Surg Forum.* 2004;7: E259-E264.
17. Whisenant B, Kapadia SR, Eleid MF, et al. One-year outcomes of mitral valve-in-valve using the SAPIEN 3 transcatheter heart valve. *JAMA Cardiol.* 2020;5:1245-1252.

SUPPORTING INFORMATION

Additional supporting information may be found in the online version of the article at the publisher's website.

How to cite this article: Wang DD, O'Neill BP, Caranasos TG, Chitwood WR Jr, Stack RS, O'Neill WW. Comparative differences of mitral valve-in-valve implantation: A new mitral bioprosthesis versus current mosaic and epic valves. *Catheter Cardiovasc Interv.* 2022;99:934-942. <https://doi.org/10.1002/ccd.30011>